A Maurer's cleft–associated protein is essential for expression of the major malaria virulence antigen on the surface of infected red blood cells

Brian M. Cooke,[1] Donna W. Buckingham,[1] Fiona K. Glenister,[1] Kate M. Fernandez,[1] Lawrence H. Bannister,[3] Matthias Marti,[4] Narla Mohandas,[5] and Ross L. Coppel[2]

[1]Molecular and Cellular Rheology Laboratory, Department of Microbiology, and [2]Department of Microbiology and Victorian Bioinformatics Consortium, Monash University, Victoria 3800, Australia
[3]Wolfson Centre for Age-Related Diseases, Guy's, King's, and St. Thomas' Hospitals School of Biomedical and Health Sciences, Kings College London, London SE1 1UL, United Kingdom
[4]The Walter and Eliza Hall Institute of Medical Research, Parkville, Victoria 3050, Australia
[5]New York Blood Center, New York, NY 10021

The high mortality of *Plasmodium falciparum* malaria is the result of a parasite ligand, PfEMP1 (*P. falciparum*) erythrocyte membrane protein 1), on the surface of infected red blood cells (IRBCs), which adheres to the vascular endothelium and causes the sequestration of IRBCs in the microvasculature. PfEMP1 transport to the IRBC surface involves Maurer's clefts, which are parasite-derived membranous structures in the IRBC cytoplasm. Targeted gene disruption of a Maurer's cleft protein, SBP1 (skeleton-binding protein 1), prevented IRBC adhesion because of the loss of PfEMP1 expression on the IRBC surface. PfEMP1 was still present in Maurer's clefts, and the transport and localization of several other Maurer's cleft proteins were unchanged. Maurer's clefts were altered in appearance and were no longer found as close to the periphery of the IRBC. Complementation of mutant parasites with s*bp1* led to the reappearance of PfEMP1 on the IRBC surface and the restoration of adhesion. Our results demonstrate that SBP1 is essential for the translocation of PfEMP1 onto the surface of IRBCs and is likely to play a pivotal role in the pathogenesis of *P. falciparum* malaria.

Introduction

Asexual stages of the malaria parasite *Plasmodium falciparum* invade and replicate in human RBCs. During the 48 h of its asexual life cycle, the parasite dramatically remodels the host RBC (for reviews see Cooke et al., 2001, 2004). This includes the generation of unique, flattened membranous structures in the cytoplasm of the infected RBC (IRBC) called Maurer's clefts and protrusions on the IRBC surface termed knobs. *P. falciparum* also exports several proteins into the host RBC by a mechanism that depends on the presence of an NH_2-terminal motif, termed either the *Plasmodium* export element (PEXEL) or vacuolar transport signal (VTS), which is conserved across the *Plasmodium* genus (Hiller et al., 2004; Marti et al., 2004). One of the most important of these exported proteins is PfEMP1 (*P. falciparum* erythrocyte membrane protein 1), a protein of parasite origin that is exposed on the surface of IRBCs and mediates adhesion to several receptors expressed on the surface of vascular endothelial cells (Baruch et al., 2002). Ultimately, this results in the adhesion of mature parasite-infected RBCs to the vascular endothelium, which is a process that underpins the development of severe and often fatal complications that accompany *P. falciparum* malaria infection in humans (MacPherson et al., 1985; Pongponratn et al., 1991). Therefore, understanding the pathways and molecular mechanisms by which parasites export proteins to the RBC membrane is critical for a complete understanding of the pathogenesis of *P. falciparum* malaria and, in the longer term, could lead to the development of novel therapeutic approaches to prevent cytoadherence and severe pathological sequelae.

For most parasite proteins that are destined for the RBC membrane skeleton and the surface, trafficking seems to involve Maurer's clefts (Przyborski et al., 2003; Marti et al., 2004;

Correspondence to Brian M. Cooke: brian.cooke@med.monash.edu.au

Abbreviations used in this paper: FRET, fluorescent resonance energy transfer; hdhfr, human dihydrofolate reductase; HRP, histidine-rich protein; HSP, heat shock protein; IFA, immunofluorescence assay; IRBC, infected RBC; KAHRP, knob-associated HRP; KO, knockout; MAHRP, Maurer's cleft–associated HRP; PEXEL, *Plasmodium* export element; PfEMP, *Plasmodium falciparum* erythrocyte membrane protein; REX, ring-stage exported protein; SBP1, skeleton-binding protein 1; VTS, vacuolar transport signal.

The online version of this article contains supplemental material.

© The Rockefeller University Press $8.00
The Journal of Cell Biology, Vol. 172, No. 6, March 13, 2006 899–908
http://www.jcb.org/cgi/doi/10.1083/jcb.200509122

Knuepfer et al., 2005). Clefts appear at the early trophozoite stage of parasite development and persist throughout the remainder of the intra-erythrocytic cycle. The final destination of Maurer's clefts in IRBCs does appear to be in juxtaposition with the RBC membrane skeleton, and there is some evidence to suggest that they may interact with actin, ankyrin, or other proteins associated with the RBC membrane skeleton such as LANCL1 (Blisnick et al., 2000, 2005). It is possible that Maurer's clefts dock with the RBC membrane skeleton and provide the exit site for proteins, such as PfEMP1, that are exposed on the surface of the IRBC; however, such a mechanism has not yet been demonstrated.

Several proteins have been described that are resident within Maurer's clefts, but there is no information about their functional roles and whether they may be involved in protein trafficking (Hawthorne et al., 2004; Vincensini et al., 2005). One of the first Maurer's cleft proteins to be described was *P. falciparum* SBP1 (skeleton-binding protein 1), a 48-kD integral membrane protein that spans the Maurer's cleft membrane (Blisnick et al., 2000). The NH_2-terminal domain is found within the cleft, whereas the COOH-terminal domain is exposed within the IRBC cytoplasm and interacts with a RBC membrane skeleton protein, possibly participating in anchoring the clefts to the RBC membrane skeleton (Blisnick et al., 2000). To determine the function of SBP1 in IRBCs, we have generated clonal transgenic parasite lines in which SBP1 is not expressed and have extensively examined the biological properties of these mutant IRBCs. Analysis of the SBP1-deleted parasite line revealed that the major virulence factor PfEMP1 is not expressed on the surface of the IRBC and that the wild-type phenotype can be restored when the gene deletion is complemented. Importantly, the SBP1-deleted parasite line (SBP1 knockout [KO]) represents the first *P. falciparum* parasite line showing a knockdown in PfEMP1 surface expression.

Results

Disruption of the SBP1 locus

sbp1 (PlasmoDB accession no. PFE0065w) is a 1.2-kb gene comprising two exons separated by a 170-bp intron and is located in the subtelomeric region of *P. falciparum* chromosome 5 (Fig. 1). To determine the function of SBP1, we disrupted the *sbp1* gene in *P. falciparum* 3D7 parasites (Fig. 2 A). Integration of the drug resistance cassette into *sbp*1 by homologous recombination would disrupt the coding region at residue 192. Eight clonal lines were selected from two independent transfection events. Of the eight selected clones, three were selected for further analysis (1G8, 2D8, and 1G5). Analysis of intact chromosomes derived from these transgenic clonal lines, which were separated by pulsed field gel electrophoresis as previously described (Kemp et al., 1985), confirmed that integration into chromosome 5 had occurred (not depicted). Analysis by Southern blotting using genomic DNA digested with ClaI and EcoRI and probed with either h*dhfr* (human dihydrofolate reductase) or *sbp1*-F2 confirmed that the *sbp1* gene had been disrupted in all three parasite clones (Fig. 2 B). No episomal plasmid could be detected in any of the clones by PCR analysis. Restriction fragments of the predicted sizes were also obtained on similar Southern blots using DNA digested with alternative endonucleases EcoRI–XhoI or NsiI (not depicted). As expected, the analysis of three selected parasite clones by Western blotting using polyclonal antibodies raised against either NH_2- or COOH-terminal regions of SBP1 (Blisnick et al., 2000) revealed that SBP1 expression had been ablated in all three transgenic clones (1G5, 1G8, and 2D8; Fig. 2 C). There was no reactivity of any of the bands with antibodies against the NH_2-terminal region of SBP1 with any of the transgenic clones, which is indicative of the loss of translation of full-length SBP1. One of the three clones (1G8) was selected for more detailed analysis. The examination of IRBCs infected with 1G8 parasites by immunofluorescence using mouse polyclonal antisera specific for SBP1 failed to show any reactivity, suggesting that there were no truncated SBP1 products and that SBP1 expression had been completely ablated (Fig. 2 D).

Immunofluorescence analysis reveals no difference in the localization of exported parasite proteins to Maurer's clefts in the SBP1 KO line compared with 3D7 wild-type parasites

Because SBP1 is known to be a major structural component of Maurer's clefts, we wanted to assess Maurer's cleft structure and function in the SBP1 KO line compared with the 3D7

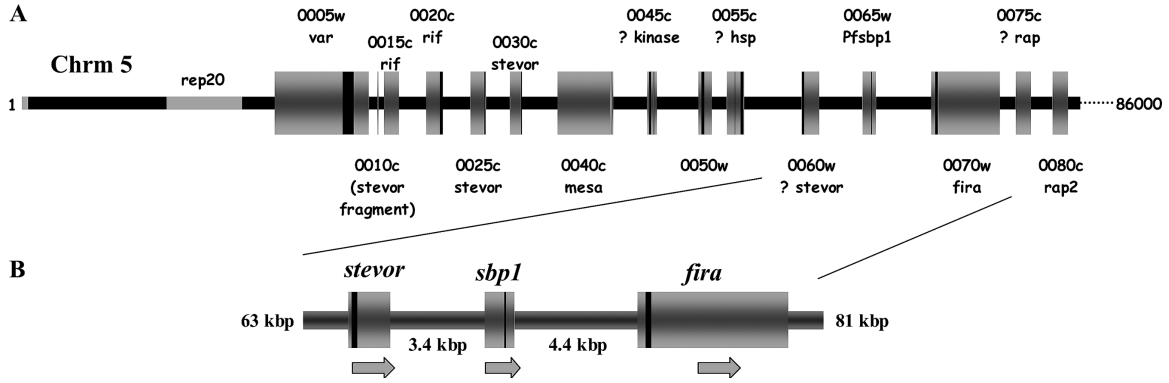

Figure 1. **Schematic representation of *P. falciparum* chromosome 5 and the *sbp1* locus.** (A) Arrangement of genes on *P. falciparum* chromosome 5 in the region between 1 and 86 kbp. (B) Expanded view of *P. falciparum* chromosome 5 between 63 and 81 kbp, indicating the position of *sbp1* and flanking genes. Arrows indicate the direction of transcription. Intragenic distances between *sbp1* and neighboring genes are indicated.

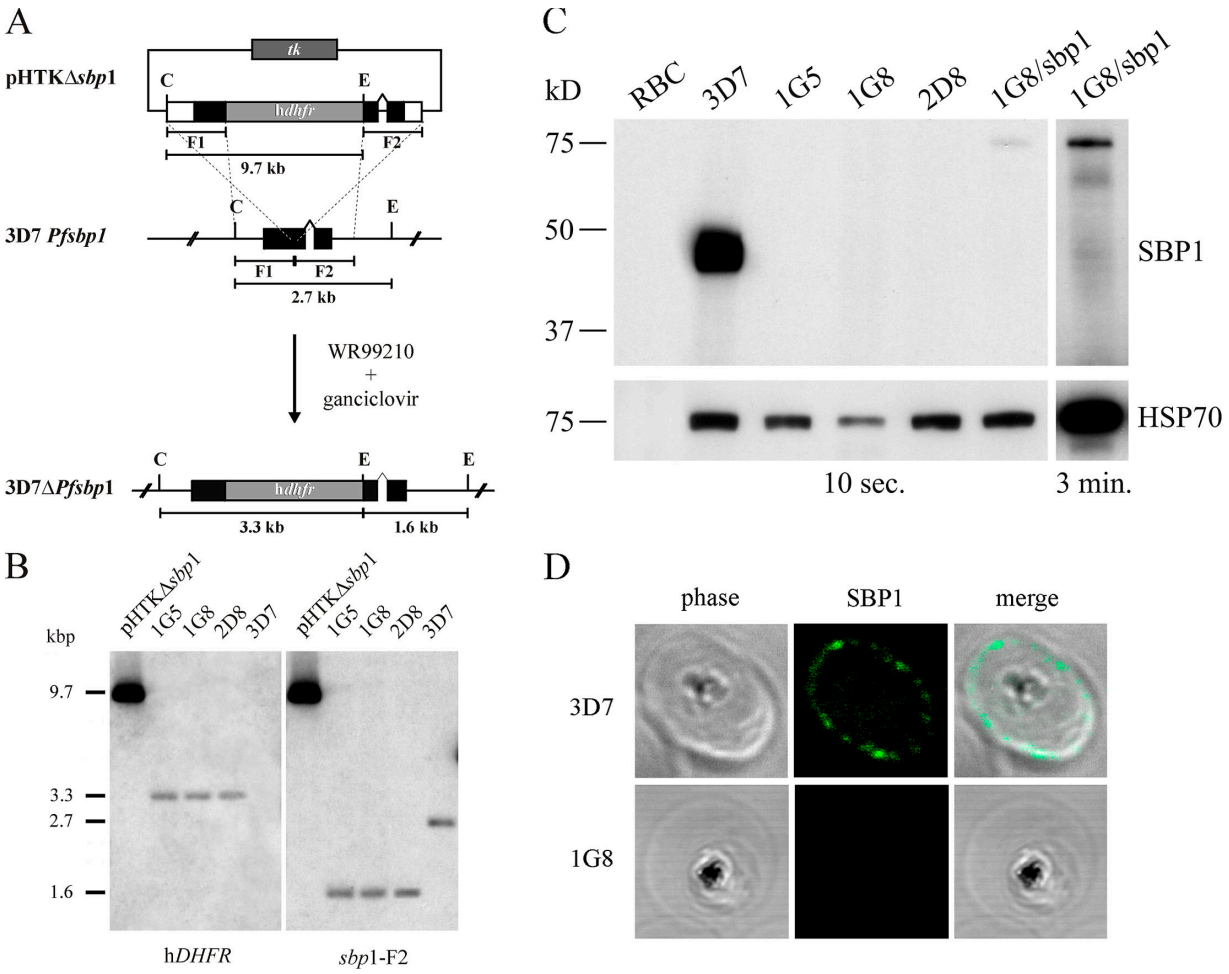

Figure 2. **Disruption of the *sbp1* gene completely abolishes SBP1 expression in IRBCs.** (A) Schematic representation of the pHTKΔ*sbp1* transfection plasmid and disruption of the *sbp1* gene (3D7*Pfsbp1*) in *P. falciparum* 3D7 parasites. The position of relevant restriction enzyme sites ClaI (C) and EcoRI (E) and the expected sizes of restriction fragments are indicated. The *sbp1* gene locus disrupted by the h*dhfr* resistance cassette in drug-resistant transfected parasites is also shown (3D7ΔPf*sbp1*). (B) Southern blot analysis of ClaI–EcoRI-digested pHTKΔ*sbp1* DNA and genomic DNA from 3D7 and three *sbp1*-deleted transgenic clones: 1G5, 1G8, and 2D8. Hybridization of the h*dhfr* and *sbp1*-F2 probes to digested DNA from all 3D7Δ*sbp1* parasite clones revealed restriction fragments consistent with the disruption of *sbp1*. (C) Western blot analysis of SBP1 expression in 3D7 parasites, *sbp1*-deleted transgenic clones (1G5, 1G8, and 2D8), and the complemented parasite line 1G8/*sbp1*. Blots were probed with an NH_2-terminal anti-SBP1 antibody (top). SBP1 is visualized as a band at ~48 kD in the parental 3D7 clonal line. In 1G8/*sbp1* parasites, SBP1 is visualized as a slower migrating protein at ~75 kD, corresponding to expression of the SBP1-EYFP chimera. Because of the lower level of SBP1-EYFP expression in complemented parasites, a longer exposure (3 min) is also shown. Blots were also probed for HSP70 as a loading control (bottom). (D) Immunofluorescence analysis of SBP1 in IRBCs infected with either 3D7 or 1G8 parasites. Note that no fluorescence associated with Maurer's clefts can be seen in the *sbp1*-deleted 1G8 parasite clone.

wild-type parasites. We first analyzed the localization of several intrinsic Maurer's cleft markers (Wickham et al., 2001; Wickert et al., 2003; Hawthorne et al., 2004) in the two parasite lines. As shown in Fig. 3 A, the deletion of SBP1 from 3D7 parasites had no apparent affect on the expression or internal cellular localization of two resident Maurer's cleft proteins, Pf332 and REX (ring-stage exported protein). In addition, we analyzed proteins that are transiently associated with Maurer's clefts. Both PfEMP1 and KAHRP (knob-associated histidine-rich protein [HRP]), the major structural component of knobs, are still present in the Maurer's clefts of the SBP1 KO line, and, within the limits of discrimination of immunofluorescence, there appears to be no gross change in the amount of either protein within Maurer's clefts (Fig. 3 B). Similarly, PfEMP3, a protein transported to the IRBC membrane skeleton, is still able to reach its customary location (not depicted). Treating IRBCs with the pore-forming agent streptolysin O, which increases antibody accessibility to Maurer's clefts, revealed similar levels of PfEMP1 colocalization with another resident Maurer's cleft marker, MAHRP (Maurer's cleft–associated HRP; Spycher et al., 2003) in both parental and SBP1 KO lines (Fig. 3 C).

SBP1 KO parasites show slightly altered Maurer's cleft location and ultrastructure, but knob formation and architecture are not affected

Examination of transmission electron micrographs of RBCs infected with either 3D7 or 1G8 parasites (Fig. 4) revealed the presence of identifiable Maurer's clefts in both types of IRBCs. Precise quantitation revealed no significant difference in the number of Maurer's clefts in 1G8 parasites when compared with 3D7 (1.28 ± 0.16 vs. 1.30 ± 0.16 clefts/μm^2; mean ± SEM for

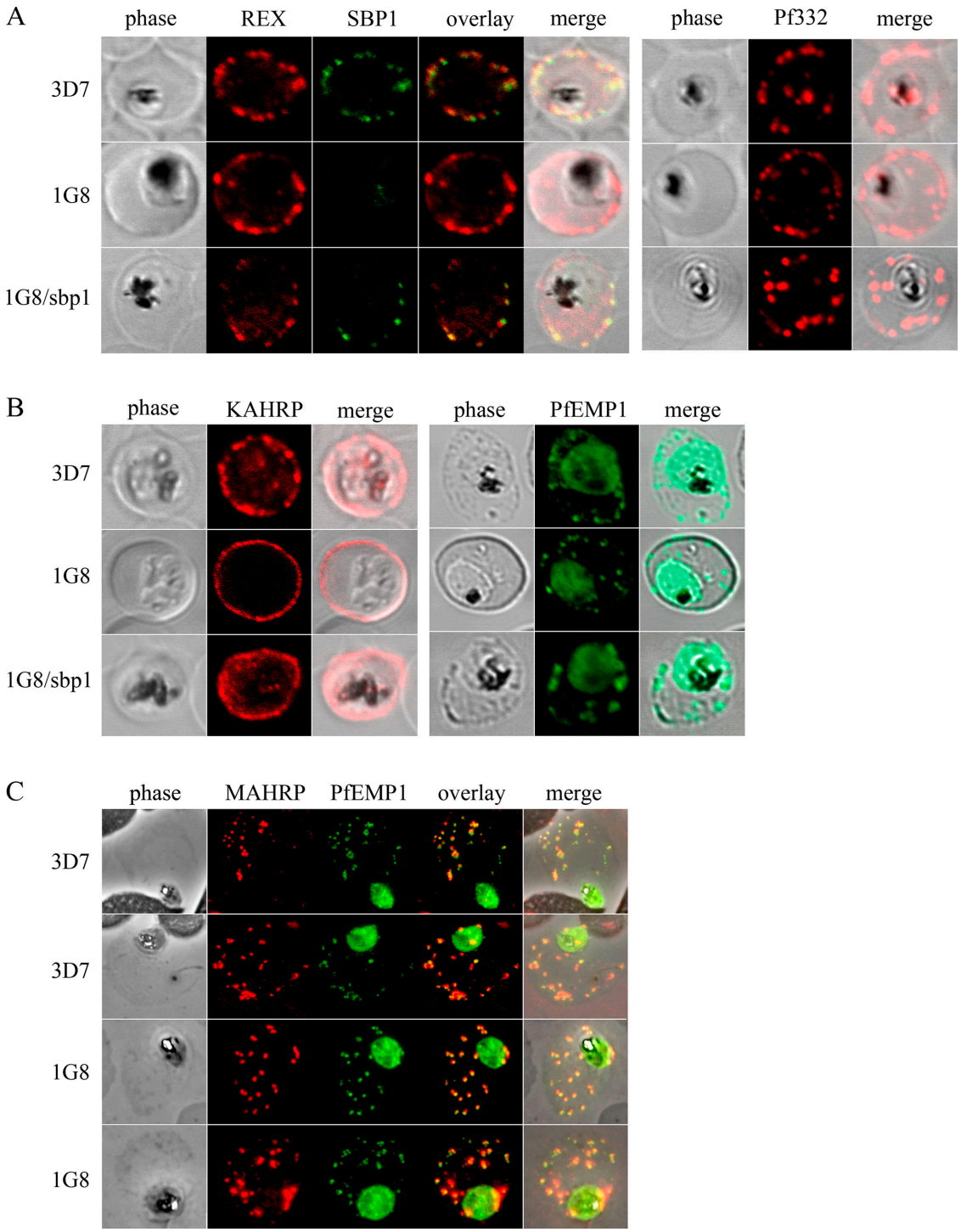

Figure 3. **Analysis of expression and localization of Maurer's cleft–associated proteins in IRBCs.** (A) Confocal immunofluorescence analysis of resident (A; REX, SBP1, and Pf332) or transiently associated (B; KAHRP and PfEMP1) Maurer's cleft proteins in normal (3D7) SBP1-deleted (1G8) and SBP1-complemented (1G8/*sbp1*) IRBCs. (C) Colocalization of the resident Maurer's cleft marker MAHRP with PfEMP1 in streptolysin O–pretreated IRBCs demonstrates that PfEMP1 is associated with Maurer's clefts in both 3D7 and SBP1-deteted parasites.

1G8 and 3D7 parasites, respectively). In both parasite lines, IRBCs with more than one parasite tended to have proportionately more clefts. In a total of 64 random IRBCs examined, only one 3D7 IRBC and one 1G8 IRBC had no detectable clefts at all. When examined at higher magnification, however, there were subtle detectable differences in the fine morphological structure of the clefts, which were typically narrower in RBCs infected with 1G8 parasites when compared with RBCs infected with 3D7 (Fig. 4, G–N). We also examined Maurer's cleft location in the parental 3D7 and KO 1G8 lines, measuring the minimum distances of the cleft from the nearest IRBC surface. In both sets of samples (number of clefts examined = 37 for each), most

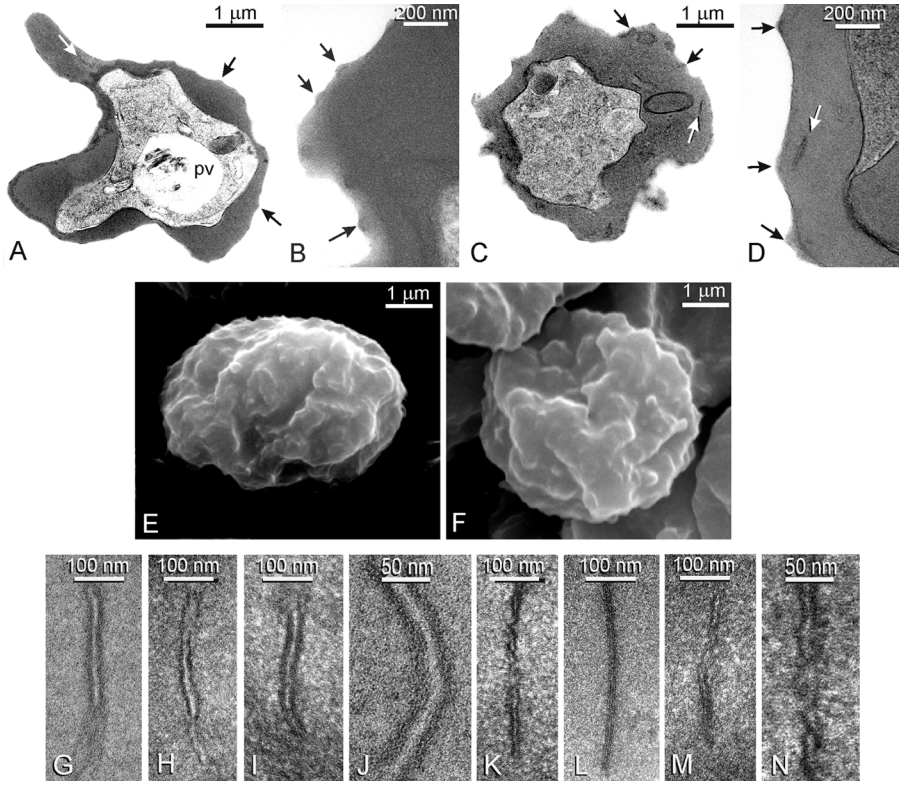

Figure 4. **Ultrastructural analysis of IRBCs.** Comparisons of Maurer's clefts and surface knob appearances in RBCs infected with wild-type 3D7 (A, B, E, and G–J) or *sbp1*-deleted 1G8 parasites (C, D, F, and K–N). Survey transmission electron micrographs of 3D7 (A and B) and 1G8 (C and D) show that both express Maurer's clefts (white arrows) and knobs (black arrows), and scanning electron microscopy of 3D7 (E) and 1G8 (F) also shows a similar expression of knobs. However, transmission electron microscopy at higher magnifications shows differences between 3D7 clefts (G–J) and those of 1G8 (K–N), in which clefts are typically narrower with a reduced intermembrane space; shown in higher magnification in J (3D7) and N (1G8). pv, pigment vacuole.

clefts were approximately parallel to the surface, and, in both, about one fifth of clefts were angled so as to approach the surface closely. The minimum distance from the cell surface to the Maurer's cleft in 3D7 IRBCs was 139 ± 12 nm (mean ± SEM), whereas in the SBP1 KO line, Maurer's clefts were on average slightly further from the IRBC surface (160 ± 15 nm).

By scanning electron microscopy, the external appearances of 3D7 or 1G8 IRBCs were similar, with irregular surfaces bearing numerous knobs (Fig. 4, E and F). The knobs on both 3D7 and 1G8 IRBCs also looked identical by transmission electron microscopy (Fig. 4, A–D; black arrows). Precise quantitation revealed that there were no significant differences between the number of knobs on 1G8 IRBCs when compared with 3D7 IRBCs (3.43 ± 0.31 vs. 3.45 ± 0.31 knobs/μm^2; mean ± SEM for 1G8 and 3D7, respectively). In both parasite lines, IRBCs with more than one parasite tended to have proportionately more knobs. In the total of 64 random IRBCs examined, only one 3D7 IRBC and one 1G8 IRBC had no detectable knobs at all.

Transport of PfEMP1 is arrested at Maurer's clefts in SBP1-deleted parasite lines

To examine the fate of PfEMP1 in detail, we performed various immunochemical and proteolytic assays on surface-exposed PfEMP1 in both parental and mutant parasite lines. It has previously been shown that PfEMP1 changes its solubility during transport to the IRBC surface. Specifically, the protein is soluble in Triton X-100 during transport in the IRBC but becomes detergent insoluble/SDS soluble when incorporated into the knob structure on the IRBC surface (Kriek et al., 2003). In addition, the large NH_2-terminal PfEMP1 exodomain is sensitive to trypsin when the protein is surface exposed (Waterkeyn et al., 2000). We analyzed the distribution of PfEMP1 in both wild-type and SBP1 KO parasites by Western blot analysis of the Triton X-100–insoluble/SDS-soluble fraction of membrane proteins with and without trypsin treatment of intact IRBCs (Fig. 5). Thus, in the parental 3D7 line, PfEMP1 was present in the Triton X-100–insoluble/SDS-soluble fraction and was cleaved after exposure to trypsin. In contrast, PfEMP1 was not present in the Triton X-100–insoluble/SDS-soluble fraction in the SBP1 KO line, and the protein was not sensitive to trypsin treatment (Fig. 5 A). To control for trypsin digestion, we examined the fate of an integral membrane and surface-exposed protein of human RBCs, glycophorin C, in both parental and mutant parasite lines. In both cases, glycophorin C was cleaved by the exogenous trypsin, demonstrating that PfEMP1 in the SBP1 KO line was not present on the IRBC surface but remained internal within the Maurer's clefts as shown by immunofluorescence assay (IFA; Fig. 3 C). The relative differences in the amount of PfEMP1 in this Triton X-100–insoluble fraction can be more readily visualized after the extensive preabsorption of anti-PfEMP1 antiserum against inside-out RBCs to reduce cross-reactivity of the antiserum with RBC spectrin (Fig. 5 B). There is almost no detectable product in the KO parasite line, suggesting that there is no intermediate compartment between residence in the Maurer's cleft and exposure on the surface. It also suggests that PfEMP1 has not exited the cleft but becomes trapped in association with the membrane skeleton en route to the IRBC surface. Together with our IFA experiments (Fig. 3), these data are consistent with a block in the surface expression of PfEMP1 at the level of the Maurer's clefts in the SBP1 KO parasite line.

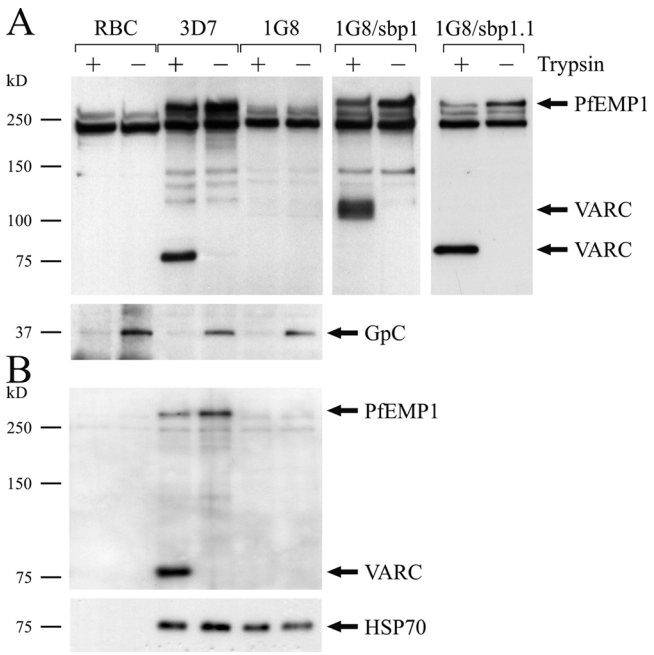

Figure 5. **Analysis of surface-exposed PfEMP1 on IRBCs by trypsin cleavage assay.** (A) Western blot analysis of Triton X-100–insoluble/SDS-soluble membrane fractions from intact, uninfected RBCs or IRBCs (3D7, 1G8, 1G8/*sbp1*, and 1G8/*sbp1.1*) either before (−) or after (+) treatment with trypsin. The two bands below full-length PfEMP1 at ~250 kD represent cross-reactivity with the RBC cytoskeletal proteins α and β spectrin. An identical blot was probed with mouse antiglycophorin C antibody (GpC) as a control for trypsin activity. An 80-kD band was detected in 3D7 parasites (VARC) representing the cytoplasmic domain of surface-exposed PfEMP1 in these IRBCs. Note the absence of this band in the *sbp1*-deleted parasite clone (1G8), confirming a lack of surface-exposed PfEMP1 in these IRBCs. The complemented 1G8/*sbp*1 parasite clone shows the reappearance of a trypsin-cleavable PfEMP1, although its cytoplasmic domain appears to be larger (~115 kD) than that detected in 3D7 parasites, suggesting surface exposure of a different CD36-binding PfEMP1 variant. Analysis of a second complemented clonal line (1G8/*sbp1.1*), which expresses the original 1G8 *var*, shows that PfEMP1 is surface exposed as indicated by the restoration of trypsin cleavage. (B) A similar blot to that shown in A but probed with anti-PfEMP1 antibody after preabsorption with inside-out RBCs to reduce spectrin cross-reactivity. The absence of full-length PfEMP1 on the surface of SBP1 KO IRBCs is notable. An identical blot was probed for HSP70 as a parasite loading control.

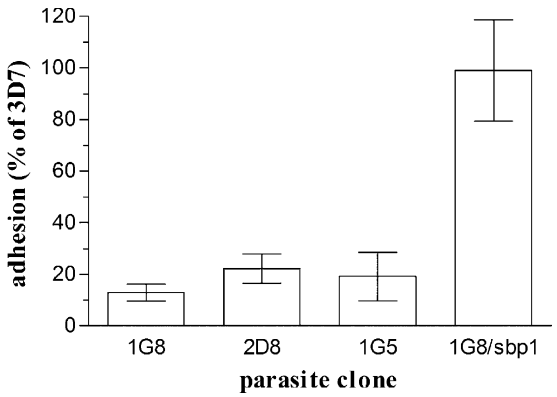

Figure 6. **Adhesive properties of IRBCs under flow conditions.** The level of adhesion of IRBCs to CD36 under flow conditions (0.1 Pa). Adhesion represents the number of IRBCs that adhered for three SBP1-deleted parasite clones (1G8, 2D8, and 1G5) as a percentage of parental 3D7 IRBCs. Note the restoration of the adhesive phenotype of the complemented 1G8/*sbp1* IRBCs back to the level of adhesion measured for the parental 3D7 line. Data represent the mean ± SEM (error bars) for five independent experiments for each parasite clone.

RBCs infected with SBP1-deleted parasites do not adhere to CD36 under static or flow conditions

Cytoadherence of IRBCs is mediated by the differential binding properties of variant PfEMP1 exodomains to several host cell receptors. The absence of PfEMP1 expression on the surface of IRBCs should, therefore, result in reduced cytoadherence in the 1G8 parasite line compared with wild-type 3D7 parasites. Because 3D7 parasites bind only to the endothelial cell surface–expressed receptor CD36, we quantified the adhesion of IRBCs to this receptor using both static and flow-based adhesion assays. In static assays, the ability of RBCs infected with 1G8 parasites to adhere was significantly reduced by >96% when compared with the level of adhesion for 3D7 IRBCs (mean reduction in adhesion = 96.7 ± 1.3%; mean ± SEM for five experiments; $P < 0.01$ by Mann-Whitney U test). Similarly, when tested under flow conditions (at 0.1 Pa), all three transgenic *sbp1*-deleted parasite clones showed significantly reduced adhesion to CD36 (Fig. 6). The low level of binding was similar for all three transgenic clones, averaging only 12% of the level for 3D7 ($P < 0.01$ by Kruskall Wallace test).

Expression of an *sbp1*-EYFP chimeric gene in 1G8 parasites restores surface PfEMP1 expression and adhesion of IRBCs to CD36

We reintroduced a full-length *sbp1* gene from 3D7 parasites under control of the constitutive *P. falciparum hsp*86 (heat shock protein 86) promotor into 1G8 parasites by transfection of the modified Gateway expression vector pHrB1-1/2 containing the 3D7 *sbp1* gene that had been amplified from cDNA and appended to the reporter protein EYFP. Examination of drug-resistant parasites by Western analysis ~80 d after transfection revealed that the resulting parasites, 1G8/*sbp1*, were clearly producing SBP1, although at a somewhat lower level than seen in wild-type parasites (Fig. 2 C). When live IRBCs were viewed under 513-nm blue light, Maurer's clefts were visualized as fluorescing structures throughout the cytoplasm of the IRBC, with a proportion of clefts in close association with the RBC membrane skeleton (Fig. 7). Analysis of these 1G8/*sbp1* parasites by immunofluorescence and confocal microscopy revealed that the SBP1-EYFP chimeric protein was trafficked correctly to Maurer's clefts that were located at the RBC membrane skeleton (Figs. 3 and 7). The SBP1-EYFP protein also colocalized with REX (Fig. 3) and other Maurer's cleft markers (Pf332 and KAHRP; not depicted), demonstrating that the SBP1-EYFP chimeric protein was being trafficked to its native cellular location.

The effect of complemented SBP1 on PfEMP1 was examined in two independent cloned lines derived from 1G8, 1G8/*sbp1*, and 1G8/*sbp1.1*. Reintroduction of SBP1 led to the reappearance of PfEMP1 on the surface of the IRBC and the restoration of cytoadherence to CD36. Surface expression could be demonstrated by the reappearance of PfEMP1 in the Triton X-100–insoluble/SDS-soluble fraction, demonstrating an association

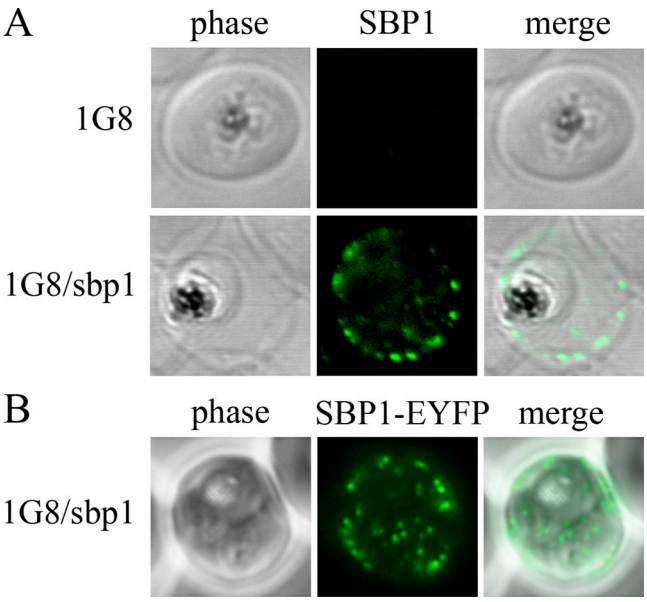

Figure 7. **Restoration of SBP1 expression by gene complementation.** (A) Immunofluorescence analysis of 1G8 and 1G8/*sbp1* IRBCs using a mouse polyclonal SBP1 (for 1G8 IRBCs) or rabbit anti-GFP polyclonal (for 1G8/*sbp1* IRBCs). Note the absence of SBP1 in the *sbp1*-deleted parasite clone 1G8 and the reappearance of SBP1 associated with Maurer's clefts that are associated with the RBC skeleton in RBCs infected with the complemented 1G8/*sbp1* parasite clone. (B) A live trophozoite-infected RBC showing green-fluorescing Maurer's clefts in the cytoplasm of a RBC parasitized by 1G8/*sbp1* parasites when viewed under 513-nm blue/green light as a result of the presence of the EYFP reporter protein appended to the COOH terminus of the chimeric *sbp*1 gene.

with the membrane skeleton (Fig. 5 A). Importantly, PfEMP1 was once again sensitive to trypsin digestion, confirming an exposed location on the IRBC surface. Of interest is that the two complemented lines derived from 1G8 differ in the variant of PfEMP1 they express on the IRBC surface. 1G8/*sbp1.1* expresses a variant of PfEMP1 that is unchanged in size from 3D7, whereas 1G8/*sbp1* has undergone a *var* gene switch to express a different variant of PfEMP1. Importantly, this demonstrates that SBP1 has a general role in PfEMP1 trafficking and is not specific to a particular PfEMP1 variant.

Reintroduction of the full-length *sbp1* gene into 1G8 parasites also dramatically restored the ability of both complemented lines to adhere to CD36 under both static and flow conditions. For example, in static assays, the reintroduction of *sbp1* into 1G8 parasites restored adhesion such that 1G8/*sbp1* IRBCs bound at levels ~60-fold higher than 1G8 IRBCs (76.1 ± 16.5% vs. 1.3 ± 1.3%; mean ± SEM for 1G8/*sbp1* and 1G8 parasite clones, respectively). Similarly, when tested under flow, adhesion of 1G8/*sbp1* IRBCs showed a level of binding similar to that measured for 3D7 IRBCs (Fig. 6). Interestingly, the 1G8/*sbp1.1* complemented line showed a consistently higher level of adhesion in both static and flow assays when compared with the wild-type 3D7 (not depicted). The amount of surface-exposed PfEMP1 that exerts this adhesive effect would appear to be quite small, as there is no detectable difference in appearance by IFA of either 1G8 or the complemented parasite lines (Fig. 3).

Discussion

Trafficking of PfE MP1 in *P. falciparum*–IRBCs has been examined by several groups recently and has been shown convincingly to occur in association with Maurer's clefts (Wickham et al., 2001; Kriek et al., 2003; Wickert et al., 2003; Marti et al., 2004; Knuepfer et al., 2005; Papakrivos et al., 2005). Exit from the parasite into the RBC cytoplasm is under the direction of a protein export motif known as the PEXEL or VTS (Hiller et al., 2004; Marti et al., 2004), and initial transport within the IRBC cytoplasm appears to be as soluble protein complexes rather than via vesicles (Kriek et al., 2003; Knuepfer et al., 2005; Papakrivos et al., 2005). PfEMP1 then appears to be inserted into the Maurer's cleft membrane, although is not clear whether the protein is transported within the cleft itself or attached to the cytoplasmic face of the cleft, as the resolution of light microscopic studies is insufficient to answer this question. Once Maurer's clefts reach the RBC membrane skeleton, PfEMP1 becomes anchored at the knob structures, and its extracellular binding domains become exposed on the RBC surface. Although it is clear that the export of PfEMP1 from the parasite to the IRBC cytoplasm is dependent on a functional PEXEL/VTS motif, it is still unknown precisely how PfEMP1 accomplishes the final translocation across the RBC membrane and what, if any, parasite or host molecules are involved in this process. It is likely that such molecules would either be present at the RBC surface, probably within the knob structure, or would be found in association with Maurer's clefts.

SBP1 has previously been shown to be a membrane protein resident in Maurer's clefts that is oriented so that its COOH-terminal domain is present in the RBC cytoplasm (Blisnick et al., 2000). Its function was previously unknown, although it has been suggested that it might be involved in binding the cleft to the RBC membrane skeleton through a specific interaction with proteins of the RBC membrane skeleton such as actin (Blisnick et al., 2000) or RBC membrane–associated proteins such as LANCL1 (Blisnick et al., 2005). SBP1 is clearly not an essential structural protein of the cleft, as its absence does not affect cleft morphology or number markedly. The subtle changes in cleft morphology related to the deletion of SBP1 noted in our studies here may merely represent the loss of SBP1 itself or the loss of a group of associated proteins that are anchored to the cleft by interaction with SBP1. We also conclude that it is not a required part of the general trafficking mechanism for parasite proteins exported to the RBC as Maurer's cleft–associated proteins because PfEMP3, Pf332, KAHRP, REX, and MAHRP are trafficked normally to the membrane skeleton of RBCs infected with *sbp1*-deleted parasites. Furthermore, the cytoadherence-related knob complexes on the surface of the IRBC form normally in *sbp1*-deleted parasite clones.

In fact, SBP1 appears to have a precise function, which is to mediate the final step in the translocation of PfEMP1 on to the surface of the IRBC. We conclude this from our observations that PfEMP1 is present in Maurer's clefts in an *sbp1*-deleted parasite line but does not appear on the surface of RBCs infected with mature stage parasites. The failure of PfEMP1 to reach the RBC surface leads to a loss of binding of IRBCs to

CD36 both in static and flow-based adhesion assays. Reintroduction of the SBP1 protein leads to the reappearance of PfEMP1 on the IRBC surface and restoration of the capacity of IRBCs to adhere to CD36. What is the mechanism by which SBP1 has this effect on PfEMP1 trafficking? Our evidence would suggest that this is not caused by a direct physical interaction between PfEMP1 and SBP1. First, analysis of the SBP1 protein sequence does not reveal any domains with homology to known protein chaperones or to proteins known to be involved in protein trafficking or vesicular transport of proteins. Second, immunoprecipitation of SBP1 from IRBC lysates does not lead to the coprecipitation of PfEMP1 (Fig. S1, available at http://www.jcb.org/cgi/content/full/jcb.200509122/DC1). Third, acceptor photobleaching fluorescent resonance energy transfer (FRET) experiments in which PfEMP1 and SBP1 were labeled with FRET-compatible fluorophores did not lead to the detectable transfer of energy from one molecule to the other (Fig. S1). This suggests that they are not found in close contact as would be expected in directly interacting proteins. Finally, a recent study devoted to the *P. falciparum* interactome reported the interactions of PfEMP1 and SBP1 with other proteins in the parasite but did not find a direct interaction between the two (LaCount et al., 2005). Collectively, these data suggest that the effect of SBP1 on PfEMP1 transport is indirect. At present, the data are most compatible with the hypothesis that the alterations in Maurer's cleft morphology and distance to the IRBC surface leads to changes that make the final translocation step of PfEMP1 markedly inefficient. These changes are subtle, and this is likely to be the reason why trafficking of only one protein, PfEMP1, is interfered with and not others such as KAHRP, which presumably have more margin for error in the relatively straightforward process of binding to nearby spectrin. In contrast, PfEMP1 must successfully perform translocation across another membrane to reach its final destination, presumably using the transmembrane and COOH-terminal domains of PfEMP1, as these have been demonstrated to be sufficient for translocation of the protein across the RBC membrane (Knuepfer et al., 2005). Whatever the ultimate mechanism, it is clear that SBP1 has a general role in PfEMP1 trafficking as surface localization of PfEMP1 is restored in complemented lines expressing variant forms of the protein.

The specific function of SBP1 in PfEMP1 translocation is consistent with its phylogenetic distribution within malaria species. We have examined several *Plasmodium spp*. genomes and are unable to identify a homologue of *sbp1* either by direct homology searching using the Basic Local Alignment Search Tool (BLAST) or Position-Specific Iterated BLAST. The *sbp1* gene is located between the genes for the exported parasite proteins *mesa* and *fira* at the subtelomeric end of chromosome 5 in *P. falciparum.* Orthology searches in the *Plasmodium* genome database (www.PlasmoDB.org) revealed that synteny between *P. falciparum* chromosome 5 and a contig from both *Plasmodium vivax* and *Plasmodium yoelii* breaks down at the *rap2* locus. This suggests that the more subtelomeric part of chromosome 5, including *fira*, *sbp1*, and *mesa*, is specific only to *P. falciparum* (Fig. 1). Other species of *Plasmodium* lack a PfEMP1-like molecule, so it is reasonable that a protein specific for translocation should also be absent from the same species. In this context, it is interesting to note that deletion of the subtelomeric end of chromosome 2 of *P. falciparum* (which frequently occurs within the *kahrp* locus) results in the loss of knobs and cytoadherence of IRBCs, although PfEMP1 is still expressed on the IRBC surface (Cooke et al., 2002c). In addition, the *kahrp* locus is also the breakpoint of synteny between *P. falciparum* chromosome 2 and a large *P. vivax* contig (Sargeant et al., 2006). This supports the idea of a few *P. falciparum*–specific subtelomeric loci that are critical for the transport and function of PfEMP1 and, consequently, in cytoadherence of IRBC to host vascular endothelium. The absence of *sbp1* in other malaria species that express proteins on the surface of the IRBC and that are involved in antigenic variation such as the *yir*, *vir*, and *kir* gene families (collectively termed the *Plasmodium* interspersed repeat superfamily [*pir*]; Janssen et al., 2004) also suggests that these molecules reach the surface of the IRBC by some other mechanism. As RIFINs are the *P. falciparum* representatives of the *pir* family in that species, it seems very likely that their trafficking to the IRBC surface in *P. falciparum* occurs by an SBP1-independent mechanism. We cannot examine this directly in our *sbp1* KO line because it is generated on a 3D7 parasite background, a line that does not express detectable RIFINs on the RBC surface (Kyes et al., 1999).

In conclusion, we show here, for the first time, that the Maurer's cleft–associated protein SBP1 plays a major role in translocation of the cytoadherence ligand PfEMP1 onto the surface of *P. falciparum*–infected RBCs. We have demonstrated this via complementation of a gene KO parasite line, which is the first study to our knowledge of the complementation of a blood stage gene in *Plasmodium spp*. Future studies will be aimed at identifying the precise mechanisms and interactions involved in this process and whether other molecular players are involved. Such knowledge might be used to interfere with the translocation process, which in vivo would be likely to be associated with a marked decrease in parasite virulence and may constitute a new therapeutic approach to the control of malaria infection in humans in the future. The availability of specific PfEMP1-null lines also makes possible new studies examining such questions as the importance of PfEMP1 in the pathogenesis of malaria by, for example, the disruption of SBP1 in monkey-adapted parasite lines and subsequent infection of primate hosts. If such parasite lines are avirulent in the vertebrate host, they could become the basis of a genetically defined attenuated vaccine for use in humans.

Materials and methods

Malaria parasites

P. falciparum parasites (3D7) were maintained in continuous in vitro culture in human RBCs suspended in Hepes-buffered RPMI 1640 supplemented with 0.5% AlbumaxII using standard procedures (Cranmer et al., 1997). Cultures were kept synchronous, and the knob-positive phenotype was maintained by gelatin floatation (Waterkeyn et al., 2001). Clonal parasite lines were derived by the method of limiting dilution.

Plasmid constructs

To disrupt the *sbp1* gene in 3D7 parasites, 5′ and 3′ sequences of ~1 kb flanking the *sbp1* gene were cloned into the *P. falciparum* transfection plasmid pHHT-TK (gift from A. Cowman and B. Crabb, The Walter and

Eliza Hall Institute, Melbourne, Australia; Duraisingh et al., 2002) to derive pHTKΔ*sbp1* (Fig. 2 A). Specifically, the 5′ segment of *sbp1* (including 458 bp of the 5′ untranslated sequence) was amplified from genomic DNA from 3D7 parasites using forward and reverse primers 5′TCCCCGCGGcgatacaaccctcctttatg3′ (SacII site underlined) and 5′GGACTAGTgacatagattcggctgga3′ (SpeI site underlined), respectively, and was subcloned into the SacII and SpeI sites of pHHT-TK upstream of the h*dhfr* resistance cassette. The 3′ segment of *sbp1* (including 437 bp of the 3′ untranslated sequence) was amplified using the forward and reverse primers 5′CGGAATTCgcagattttgcaaaacaagc3′ (EcoRI site underlined) and 5′CATGCCATGGcatatacataaacgatcaaaag3′ (NcoI site underlined), respectively, and was introduced into the EcoRI and NcoI sites downstream of the h*dhfr* cassette. Plasmid DNA was amplified in *Escherichia coli* and purified using MegaPrep (QIAGEN).

For complementation, the full-length *sbp1* gene (excluding the stop codon) was PCR amplified from 3D7 cDNA using the forward and reverse primers 5′CACCTATATACAatgtgtagcgcagctcgagca3′ and ggtttctctagcaactgtttttg, respectively, and was cloned using topoisomerase into the multisite Gateway entry vector pENTR/D-TOPO (Invitrogen). This was recombined together with pDONR P4-P1R vector containing the *P. falciparum Hsp86* promoter and pDONR P2R-P3 vector containing the EYFP reporter gene into a destination vector, pHrB1-1/2, that had been previously modified for use in *P. falciparum* (van Dooren et al., 2005) to produce the expression plasmid pHrB1-1/2-*sbp1*.

Parasite transfection

Ring-stage parasites were transfected by electroporation with 150 μg of purified supercoiled plasmid DNA (pHTkΔ*sbp1*) diluted in cytomix according to standard procedures (Wu et al., 1996) but using modified electroporation conditions to enhance DNA delivery (Fidock and Wellems, 1997). Transfected parasites were cultured in the presence of 2.5 nM of the antifolate drug WR99210 (Fidock and Wellems, 1997) for ~30 d until viable parasites were observed in Giemsa-stained smears. 4 μM ganciclovir (Roche Diagnostics) was then added to select for parasites having only double crossover homologous recombination (Duraisingh et al., 2002). For complementation, positive selection for parasites transformed with pHrB1-1/2-*sbp1* was performed using 8 μM blasticidin S hydrochloride (Calbiochem) as previously described (Mamoun et al., 1999).

DNA extraction and Southern blotting

Genomic DNA was extracted from parasite culture using the Nucleon BACC2 kit (GE Healthcare), digested with ClaI and EcoRI, separated on 1% agarose gels, and transferred to nylon membranes. Southern blot hybridization was performed using standard procedures.

Western blotting

Cultured IRBCs were harvested on Percoll and solubilized in 2× reducing SDS sample buffer containing protease inhibitor cocktail (Roche Diagnostics). These total parasite extracts were separated on 10% SDS-PAGE gels and transferred to polyvinylidene difluoride (PVDF) membranes. Membranes were probed with rabbit polyclonal anti-HSP70 (1:10,000), mouse polyclonal anti-SBP1 (1:400), or mouse monoclonal antiglycophorin C (1:500; Sigma-Aldrich) antibodies. Detection by enhanced chemiluminescence (Lumi-light Western blotting substrate; Roche Diagnostics) was performed after secondary detection with either sheep anti–rabbit or sheep anti–mouse Ig-HRP conjugate (1:2,000; Silenus).

Analysis of PfEMP1 expression on the surface of IRBCs by trypsin cleavage assay

The trypsin cleavage assay was performed as previously described (Waterkeyn et al., 2000) to visualize PfEMP1 expressed on the IRBC surface. In brief, mature IRBCs were enriched on Percoll as previously described (Dluzewski et al., 1984) and were incubated with 100 μg/ml TPCK-treated trypsin (Sigma-Aldrich) in the presence or absence of 1 mg/ml soybean trypsin inhibitor (STI; Sigma-Aldrich) for 15 min at 37°C. Reactions were stopped by the addition of STI to a final concentration of 1 mg/ml followed by a further incubation of 15 min at room temperature. Membrane proteins (including PfEMP1) were extracted using Triton X-100 and SDS solubilization as described previously (Van Schravendijk et al., 1993) and diluted in reducing Laemmli sample buffer. Samples were separated on 6% SDS-PAGE gels and transferred for 4 h at 4°C onto PVDF membranes. The cytoplasmic tail of PfEMP1 (VARC) was detected using the mouse monoclonal antibody 1B/98-6H1-1 (1:100; gift from The Walter and Eliza Hall Institute).

Fluorescence and confocal microscopy

For indirect immunofluorescence, cultured RBCs were fixed in suspension with 4% PFA containing 0.0075% glutaraldehyde in PBS, permeabilized with 0.1% Triton X-100, and blocked with 3% BSA in PBS as previously described (Tonkin et al., 2004). Cells were then incubated for 1 h with either mouse polyclonal anti-SBP1 (1:500), rabbit polyclonal anti-KAHRP (1:500), rabbit polyclonal anti-Pf332 (1:200), rabbit polyclonal anti–REX-1 (1:2,000; gift from D. Gardiner, Queensland Institute of Medical Research, Brisbane, Australia), mouse polyclonal anti–MAHRP-1 (1:200; gift from C. Spycher and H.-P. Beck, Swiss Tropical Institute, Basel, Switzerland), or rabbit polyclonal anti-GFP (1:1.000; Invitrogen). For PfEMP1 localization using rabbit polyclonal anti-VARC (1:100), detection was performed using thin culture smears that had been air dried and fixed with cold acetone/methanol (9:1) because this antibody showed poor reactivity when used on RBCs that had been fixed with PFA/glutaraldehyde in suspension using the method of Tonkin et al. (2004). Primary antibodies were then detected using either anti–mouse or anti–rabbit IgG conjugated to AlexaFluor488 or -568 (Invitrogen) and visualized using a laser-scanning confocal microscope (model TCS NT; Leica) equipped with a krypton/argon laser (488/568 nm). The confocal scan head was mounted on an inverted microscope (model DM RBE; Leica) equipped with a 100× NA 1.4 oil plan-Apo objective. All images of individual RBCs shown in figures are representative of numerous similar RBCs in multiple fields of view. Green fluorescence of EYFP-expressing transformants was observed using live unfixed RBCs directly from culture under 513-nm light using a fluorescence microscope (BX51; Olympus).

Morphometric analysis of knobs and Maurer's clefts by electron microscopy

RBCs from synchronous cultures containing predominantly mature stage parasites (late trophozoites/young schizonts) were fixed by the dilution of packed RBCs into isotonic PBS containing 2.5% (vol/vol) electron microscopy grade glutaraldehyde (Sigma-Aldrich). After routine preparative procedures (Bannister et al., 2003), ultrathin sections were prepared for transmission electron microscopy and pelleted for SEM. Random images of IRBCs were captured digitally at a magnification of 20,000× in an electron microscope (H7600; Hitachi) and analyzed using Scion Image software (v4.0.2). Electron-dense knobs and Maurer's clefts were counted manually for each IRBC. A total of 32 IRBCs were examined for each of the parasite lines 3D7 and 1G8. Parameters measured were (1) the perimeter of each IRBC, (2) the total sectional area of each IRBC, and (3) the sectional area of the parasite (if more than one parasitewas present, their areas were added together). From the second and third parameters, the area of IRBC external to the parasite was obtained by subtraction. Knobs and Maurer's clefts were counted manually to determine their frequencies.

IRBC adhesion assays

The adhesive properties of IRBCs were quantified using both static and flow-based assays. Parasite cultures were tested when the majority of parasites were pigmented trophozoites as assessed by Giemsa-stained smears. Cultured RBCs were resuspended in adhesion buffer (Hepes-buffered RPMI 1640 supplemented with 1% BSA and pH adjusted to 7.0) to a concentration of $\sim 3 \times 10^8$ RBCs/ml for static adhesion assays or 1.5×10^8 RBCs/ml for flow-based assays. For all adhesion assays, the parasitemia averaged ~4.4% trophozoites (range of 2.2–7.8%). Static assays were performed in 36-mm petri dishes as previously described (Beeson et al., 1998) except that purified recombinant CD36 (R&D Systems) was immobilized as the target receptor (100 μg/ml). Adhesion to CD36 under flow conditions that mimic those in postcapillary venules was visualized and quantified in vitro by direct microscopic observation on a microscope (IMT-2; Olympus) with a 40× water immersion objective (Olympus) using flat, rectangular glass microcapillary tubes (Microslides; VitroCom, Inc.) connected to a flow-control system as previously described (Cooke et al., 2002a,b).

Online supplemental material

Fig. S1 shows the results from immunoprecipitation and FRET experiments to demonstrate that there is no direct molecular interaction between SBP1 and PfEMP1 in IRBCs infected with 3D7 parasites. Supplemental text provides details of these FRET and immunoprecipitation experiments. Online supplemental material is available at http://www.jcb.org/cgi/content/full/jcb.200509122/DC1.

We thank Catherine Braun-Breton (University Montpellier, Montpellier, France), Brendan Crabb, and Alan Cowman for providing antibodies, plasmids, and helpful advice. Emma Toulman cloned the full-length 3D7 *sbp1* gene for complementation experiments, and John M. Hopkins assisted with electron microscopy.

We acknowledge financial support from the National Health and Medical Research Council (NHMRC) of Australia, the National Institutes of Health (grants DK32094 and AI44008), and the Wellcome Trust (grant 069515). B.M. Cooke is an NHMRC Senior Research Fellow.

Submitted: 20 September 2005
Accepted: 6 February 2006

References

Bannister, L.H., J.M. Hopkins, A.R. Dluzewski, G. Margos, I.T. Williams, M.J. Blackman, C.H. Kocken, A.W. Thomas, and G.H. Mitchell. 2003. *Plasmodium falciparum* apical membrane antigen 1 (PfAMA-1) is translocated within micronemes along subpellicular microtubules during merozoite development. *J. Cell Sci.* 116:3825–3834.

Baruch, D.I., S.J. Rogerson, and B.M. Cooke. 2002. Asexual blood stages of malaria antigens: cytoadherence. *Chem. Immunol.* 80:144–162.

Beeson, J.G., W. Chai, S.J. Rogerson, A.M. Lawson, and G.V. Brown. 1998. Inhibition of binding of malaria-infected erythrocytes by a tetradecasaccharide fraction from chondroitin sulfate A. *Infect. Immun.* 66:3397–3402.

Blisnick, T., M.E. Morales Betoulle, J.C. Barale, P. Uzureau, L. Berry, S. Desroses, H. Fujioka, D. Mattei, and C. Braun Breton. 2000. *Pfsbp1*, a Maurer's cleft *Plasmodium falciparum* protein, is associated with the erythrocyte skeleton. *Mol. Biochem. Parasitol.* 111:107–121.

Blisnick, T., L. Vincensini, J.C. Barale, A. Namane, and C. Braun Breton. 2005. LANCL1, an erythrocyte protein recruited to the Maurer's clefts during *Plasmodium falciparum* development. *Mol. Biochem. Parasitol.* 141:39–47.

Cooke, B.M., N. Mohandas, and R.L. Coppel. 2001. The malaria-infected red blood cell: structural and functional changes. *Adv. Parasitol.* 50:1–86.

Cooke, B.M., R.L. Coppel, and G.B. Nash. 2002a. Analysis of the adhesive properties of *Plasmodium falciparum*-infected red blood cells under conditions of flow. *Methods Mol. Med.* 72:561–569.

Cooke, B.M., R.L. Coppel, and G.B. Nash. 2002b. Preparation of adhesive targets for flow-based cytoadhesion assays. *Methods Mol. Med.* 72:571–579.

Cooke, B.M., F.K. Glenister, N. Mohandas, and R.L. Coppel. 2002c. Assignment of functional roles to parasite proteins in malaria-infected red blood cells by competitive flow-based adhesion assay. *Br. J. Haematol.* 117:203–211.

Cooke, B.M., N. Mohandas, and R.L. Coppel. 2004. Malaria and the red blood cell membrane. *Semin. Hematol.* 41:173–188.

Cranmer, S.L., C. Magowan, J. Liang, R.L. Coppel, and B.M. Cooke. 1997. An alternative to serum for cultivation of *Plasmodium falciparum* in vitro. *Trans. R. Soc. Trop. Med. Hyg.* 91:363–365.

Dluzewski, A.R., I.T. Ling, K. Rangachari, P.A. Bates, and R.J.M. Wilson. 1984. A simple method for isolating viable mature parasites of *Plasmodium falciparum* from cultures. *Trans. R. Soc. Trop. Med. Hyg.* 78:622–624.

Duraisingh, M.T., T. Triglia, and A.F. Cowman. 2002. Negative selection of *Plasmodium falciparum* reveals targeted gene deletion by double crossover recombination. *Int. J. Parasitol.* 32:81–89.

Fidock, D.A., and T.E. Wellems. 1997. Transformation with human dihydrofolate reductase renders malaria parasites insensitive to WR99210 but does not affect the intrinsic activity of proguanil. *Proc. Natl. Acad. Sci. USA*. 94:10931–10936.

Hawthorne, P.L., K.R. Trenholme, T.S. Skinner-Adams, T. Spielmann, K. Fischer, M.W. Dixon, M.R. Ortega, K.L. Anderson, D.J. Kemp, and D.L. Gardiner. 2004. A novel *Plasmodium falciparum* ring stage protein, REX, is located in Maurer's clefts. *Mol. Biochem. Parasitol.* 136:181–189.

Hiller, N.L., S. Bhattacharjee, C. van Ooij, K. Liolios, T. Harrison, C. Lopez-Estrano, and K. Haldar. 2004. A host-targeting signal in virulence proteins reveals a secretome in malarial infection. *Science*. 306:1934–1937.

Janssen, C.S., R.S. Phillips, C.M. Turner, and M.P. Barrett. 2004. *Plasmodium* interspersed repeats: the major multigene superfamily of malaria parasites. *Nucleic Acids Res.* 32:5712–5720.

Kemp, D.J., L.M. Corcoran, R.L. Coppel, H.D. Stahl, A.E. Bianco, G.V. Brown, and R.F. Anders. 1985. Size variation in chromosomes from independent cultured isolates of *Plasmodium falciparum. Nature*. 315:347–350.

Kenworthy, A.K. 2001. Imaging protein-protein interactions using fluorescence resonance energy transfer microscopy. *Methods*. 24:289–296.

Knuepfer, E., M. Rug, N. Klonis, L. Tilley, and A.F. Cowman. 2005. Trafficking of the major virulence factor to the surface of transfected *P. falciparum*-infected erythrocytes. *Blood*. 105:4078–4087.

Kriek, N., L. Tilley, P. Horrocks, R. Pinches, B.C. Elford, D.J. Ferguson, K. Lingelbach, and C.I. Newbold. 2003. Characterization of the pathway for transport of the cytoadherence-mediating protein, PfEMP1, to the host cell surface in malaria parasite-infected erythrocytes. *Mol. Microbiol.* 50:1215–1227.

Kyes, S.A., J.A. Rowe, N. Kriek, and C.I. Newbold. 1999. Rifins: a second family of clonally variant proteins expressed on the surface of red cells infected with *Plasmodium falciparum*. *Proc. Natl. Acad. Sci. USA*. 96:9333–9338.

LaCount, D.J., M. Vignali, R. Chettier, A. Phansalkar, R. Bell, J.R. Hesselberth, L.W. Schoenfeld, I. Ota, S. Sahasrabudhe, C. Kurschner, et al. 2005. A protein interaction network of the malaria parasite *Plasmodium falciparum. Nature*. 438:103–107.

MacPherson, G.G., M.J. Warrell, N.J. White, S. Looareesuwan, and D.A. Warrell. 1985. Human cerebral malaria. A quantitative ultrastructural analysis of parasitized erythrocyte sequestration. *Am. J. Pathol.* 119:385–401.

Mamoun, C.B., I.Y. Gluzman, S. Goyard, S.M. Beverley, and D.E. Goldberg. 1999. A set of independent selectable markers for transfection of the human malaria parasite *Plasmodium falciparum*. *Proc. Natl. Acad. Sci. USA*. 96:8716–8720.

Marti, M., R.T. Good, M. Rug, E. Knuepfer, and A.F. Cowman. 2004. Targeting malaria virulence and remodeling proteins to the host erythrocyte. *Science*. 306:1930–1933.

Papakrivos, J., C.I. Newbold, and K. Lingelbach. 2005. A potential novel mechanism for the insertion of a membrane protein revealed by a biochemical analysis of the *Plasmodium falciparum* cytoadherence molecule PfEMP-1. *Mol. Microbiol.* 55:1272–1284.

Pongponratn, E., M. Riganti, B. Punpoowong, and M. Aikawa. 1991. Microvascular sequestration of parasitized erythrocytes in human *falciparum* malaria: a pathological study. *Am. J. Trop. Med. Hyg.* 44:168–175.

Przyborski, J.M., H. Wickert, G. Krohne, and M. Lanzer. 2003. Maurer's clefts —a novel secretory organelle? *Mol. Biochem. Parasitol.* 132:17–26.

Sargeant, T.J., M. Marti, K. Simpson, E. Caler, J.M. Carlton, T. Speed, and A.F. Cowman. 2006. Lineage-specific expansion of proteins exported from malaria parasites to host erythrocytes. *Genome Biol*. In press.

Spycher, C., N. Klonis, T. Spielmann, E. Kump, S. Steiger, L. Tilley, and H.P. Beck. 2003. MAHRP-1, a novel *Plasmodium falciparum* histidine-rich protein, binds ferriprotoporphyrin IX and localizes to the Maurer's clefts. *J. Biol. Chem.* 278:35373–35383.

Tonkin, C.J., G.G. van Dooren, T.P. Spurck, N.S. Struck, R.T. Good, E. Handman, A.F. Cowman, and G.I. McFadden. 2004. Localization of organellar proteins in *Plasmodium falciparum* using a novel set of transfection vectors and a new immunofluorescence fixation method. *Mol. Biochem. Parasitol.* 137:13–21.

Topolska, A.E., A. Lidgett, D. Truman, H. Fujioka, and R.L. Coppel. 2004. Characterization of a membrane-associated rhoptry protein of *Plasmodium falciparum. J. Biol. Chem.* 279:4648–4656.

van Dooren, G.G., M. Marti, C.J. Tonkin, L.M. Stimmler, A.F. Cowman, and G.I. McFadden. 2005. Development of the endoplasmic reticulum, mitochondrion and apicoplast during the asexual life cycle of *Plasmodium falciparum. Mol. Microbiol.* 57:405–419.

Van Schravendijk, M.R., B.L. Pasloske, D.I. Baruch, S.M. Handunnetti, and R.J. Howard. 1993. Immunochemical characterization and differentiation of two approximately 300-kD erythrocyte membrane-associated proteins of *Plasmodium falciparum*, PfEMP1 and PfEMP3. *Am. J. Trop. Med. Hyg.* 49:552–565.

Vincensini, L., S. Richert, T. Blisnick, A. Van Dorsselaer, E. Leize-Wagner, T. Rabilloud, and C. Braun Breton. 2005. Proteomic analysis identifies novel proteins of the Maurer's clefts, a secretory compartment delivering *Plasmodium falciparum* proteins to the surface of its host cell. *Mol. Cell. Proteomics*. 4:582–593.

Waterkeyn, J.G., M.E. Wickham, K.M. Davern, B.M. Cooke, R.L. Coppel, J.C. Reeder, J.G. Culvenor, R.F. Waller, and A.F. Cowman. 2000. Targeted mutagenesis of *Plasmodium falciparum* erythrocyte membrane protein 3 (PfEMP3) disrupts cytoadherence of malaria-infected red blood cells. *EMBO J.* 19:2813–2823.

Waterkeyn, J.G., A.F. Cowman, and B.M. Cooke. 2001. *Plasmodium falciparum*: gelatin enrichment selects for parasites with full-length chromosome 2. Implications for cytoadhesion assays. *Exp. Parasitol.* 97:115–118.

Wickert, H., F. Wissing, K.T. Andrews, A. Stich, G. Krohne, and M. Lanzer. 2003. Evidence for trafficking of PfEMP1 to the surface of *P. falciparum*-infected erythrocytes via a complex membrane network. *Eur. J. Cell Biol.* 82:271–284.

Wickham, M.E., M. Rug, S.A. Ralph, N. Klonis, G.I. McFadden, L. Tilley, and A.F. Cowman. 2001. Trafficking and assembly of the cytoadherence complex in *Plasmodium falciparum*-infected human erythrocytes. *EMBO J.* 20:5636–5649.

Wu, Y., L.A. Kirkman, and T.E. Wellems. 1996. Transformation of *Plasmodium falciparum* malaria parasites by homologous integration of plasmids that confer resistance to pyrimethamine. *Proc. Natl. Acad. Sci. USA*. 93:1130–1134.